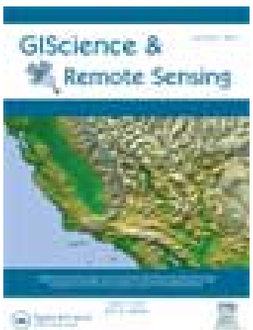

GIScience & Remote Sensing

ISSN: 1548-1603 (Print) 1943-7226 (Online) Journal homepage: http://www.tandfonline.com/loi/tgrs20

Inundation Extent and Flood Frequency Mapping Using LANDSAT Imagery and Digital Elevation Models

Shuhua Qi , Daniel G. Brown , Qing Tian , Luguang Jiang , Tingting Zhao & Kathleen M. Bergen

To cite this article: Shuhua Qi , Daniel G. Brown , Qing Tian , Luguang Jiang , Tingting Zhao & Kathleen M. Bergen (2009) Inundation Extent and Flood Frequency Mapping Using LANDSAT Imagery and Digital Elevation Models, GIScience & Remote Sensing, 46:1, 101-127

To link to this article: http://dx.doi.org/10.2747/1548-1603.46.1.101

Inundation Extent and Flood Frequency Mapping Using LANDSAT Imagery and Digital Elevation Models

Shuhua Qi
School of Geography and Environment, Jiangxi Normal University, Nanchang, Jiangxi 330027, China

Daniel G. Brown[1] and Qing Tian
School of Natural Resources and Environment, University of Michigan, 440 Church Street, Ann Arbor, Michigan 48109-1041

Luguang Jiang
Institute of Geographic Sciences and Natural Resources Research, Chinese Academy of Sciences, Beijing 100101, China

Tingting Zhao
Department of Geography, Florida State University, Tallahassee, Florida 32306-2190

Kathleen M. Bergen
School of Natural Resources and Environment, University of Michigan, 440 Church Street, Ann Arbor, Michigan 48109-1041

Abstract: We modeled the extent of inundation around Poyang Lake, China using 13 Landsat images and two digital elevation models (DEMs). Boundaries of the observed inundation extents were (a) labeled with lake-level measurements taken at a representative hydrological station and (b) interpolated to create a Water Line DEM (WL-DEM) that was used to map inundation frequency. A 30 m contour-based DEM produced slightly better results than the Shuttle Radar Topography Mission DEM, but neither DEM was accurate for medium and low lake levels. The WL-DEM exhibited improved accuracy at medium lake levels, but had relatively high errors at low lake levels.

INTRODUCTION

Lake floodplains are important environments that: (a) serve as irreplaceable habitat for many kinds of waterbirds and other animals (e.g., amphibians), because their wetlands provide abundant food and shelter; and (b) provide storage for flood waters,

[1]Corresponding author; email: danbrown@umich.edu

GIScience & Remote Sensing, 2009, **46**, No. 1, p. 101–127. DOI: 10.2747/1548-1603.46.1.101

thereby reducing the magnitudes of floods. These floodplains, often under the control of built infrastructure (i.e., levees or dams), have been exploited worldwide for food production, reducing these benefits and making agricultural production and associated human settlements vulnerable to flood damage. Knowledge of the spatial and temporal patterns of flooding, as influenced by the combination of natural flood regimes and human-built controls, is critical in maintaining the ecological functioning of floodplains (Townsend and Walsh, 1998) and predicting the pattern of flood risk facing the human populations around a lake.

Flood-risk mapping is often the first step for flood-risk management (Plate, 2002), and provides needed data for settlement planning, wildlife habitat conservation planning, design of infrastructure, and flood mitigation and response planning. Risk analysis yields hazard or risk maps, which can be created using geographic information systems (GIS) based on hydrological observations of the frequency, magnitude, and duration of flood events, as well as digital elevation models (DEMs) that characterize the topographic basin within which flood events occur. Flood-risk maps can be used to identify the weaknesses in a flood defense system and the patterns of vulnerability of human infrastructure and wildlife habitat. Because of increasing population densities in flood-prone areas throughout the world, including monsoon Asia, as well as land use and climate changes that affect flood dynamics, and the combination of these in historically less information-rich developing countries, efficient food-risk mapping is an increasingly critical tool.

DEMs have been used in various ways to aid flood mapping and modeling. They have been used as integral parts of GIS databases aiming at hydrological flood modeling (Correia et al., 1998) and for modeling the spatial extent of inundation. However, DEMs are often unavailable or of poor quality (i.e., resolution and accuracy) relative to needs for modeling, especially in developing countries. Availability has been improved with the completion of the Shuttle Radar Topography Mission (SRTM), an international research effort that obtained DEMs for nearly the entire globe. SRTM consisted of a radar system that flew on board the Space Shuttle Endeavour during an 11-day mission in February of 2000 (Rabus et al., 2003). SRTM may be used for inundation modeling, but, similar to other DEMs, special attention needs to be paid to the quality of inundation models based on DEMs in any given situation (Sanders, 2007). Because of the characteristic shallow terrain of most floodplains, DEM errors, resolution, or degree of generalization can make it difficult to use DEM-based models to successfully describe the detailed geomorphology and flood dynamics for floodplains (Lee et al., 1992; Hunter and Goodchild, 1995). The waterlines from remote sensing images have also been used to create DEMs (Smith and Bryan, 2007; Kim et al., 2007; Niedermeier et al., 2005). We refer to a DEM created from observed water elevations as a Water Line DEM (WL-DEM).

Satellite-based remote sensing images have been used to map the extent of flood inundation since the early 1970s (Deutsch et al., 1973; Rango and Solomonson, 1974). Most of the early studies used optical remote sensors, such as LANDSAT MSS and TM (Rango et al., 1974; Bhavsar, 1984; Wang et al., 2002). More recent studies have used radar sensors in place of, or in addition to, optical sensors (Townsend and Walsh, 1998; Sanyal and Lu, 2004; Andreoli et al., 2007). Because optical sensors cannot penetrate clouds, which nearly always accompany flood events, they have been mainly used to observe post-flood inundation extent (Marco et al., 2006).

Optical images also have limited ability to detect water beneath vegetation canopies with partial or complete vegetation coverage, but they have advantages of relatively fine spatial resolution (in the case of the series of sensors on Landsat and SPOT) or higher repeat frequency (in the case of AVHRR and MODIS) that make them useful in hydrological process studies (Islam and Sado, 2000; Peng et al., 2005). Combining DEMs with satellite observations of inundation extent offers a promising approach to characterizing the spatial and temporal patterns of flood risk (Sanyal and Lu, 2005).

Focusing on Poyang Lake, which is in the Central Yangtze Basin, China, we evaluated the potential of available digital elevation data, in combination with data on historical lake-level records and a suite of Landsat TM/ETM+ images, to serve as the basis for flood-risk analysis. We: (1) extracted the inundated extents from 13 Landsat TM/ETM+ images, obtained at different times with different lake levels, and developed functional relationships between inundated area and lake level for several hydrological stations to select the gauging station that best represented the dynamics for all of Poyang Lake; (2) compared maps of inundated extent derived from two DEMs, a contour-based DEM and SRTM-DEM, with remote sensing classification results to assess their accuracy; (3) created a WL-DEM using remotely sensed inundated areas, labeled with the lake-level elevations recorded on the days the images were taken, and compared the accuracy of WL-DEM–based inundation to those of the DEM-based inundations; and (4) produced flood frequency maps based on the WL-DEM and on exceedance probabilities of lake levels as measured at the most representative gauging station. The WL-DEM and flood frequency maps also provide a basis for our future work on bird habitat modeling because the spatial pattern of the vegetation around Poyang Lake is associated with elevation gradients, and different flood inundation frequencies and durations.

STUDY AREA

The study region for this research is the area around Poyang Lake, which is located in Jiangxi Province, China (Fig. 1), which we refer to as the Poyang Lake Region (PLR) in this article. The PLR includes 12 counties and has an area of 20,290 km^2. Poyang Lake is the largest freshwater lake in China, collects water from five rivers (i.e., Ganjiang, Xiushui, Fuhe, Xinjiang, and Raohe), and discharges to the Yangtze River along its central reach near the city of Jiujiang. Lake levels at the Duchang gauging station have experienced fluctuations from an average annual low (1955–2000) of 7.6 m above mean sea level (amsl)[2] in the winter to an average annual high of 17.3 m amsl in the wetter summer months (Fig. 2), resulting in lake surface-area fluctuations from <1,000 km^2 to >4,000 km^2 (Shankman and Liang, 2003). There are several small water bodies, or sub-lakes, in the basin that are hydrologically connected with the main lake when lake levels are high, but become disconnected when lake levels are low.

Water levels are important determinants of ecological and social processes within the PLR. Liu and Ye (2000) found that the spatial pattern of the vegetation around Poyang Lake corresponds to elevation gradients and different flood inundation

[2]All elevations in this paper are reported relative to the National Vertical Datum of China [NVDC], established in 1985.

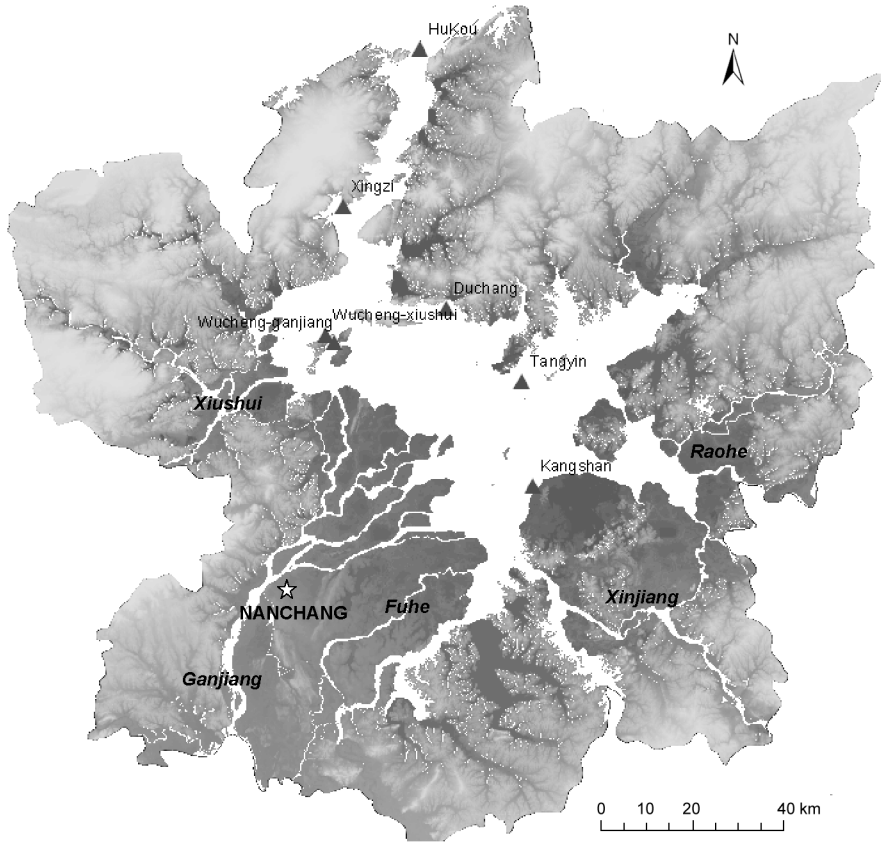

Fig. 1. Poyang Lake Region (PLR) represented by DEM (lighter shades of grey are higher elevations) and maximum free water surface (in white). Locations of gauging stations are indicated by triangles and river names are indicted in italics.

frequencies and durations. The migratory waterbirds that over-winter at Poyang Lake, many of which are listed as threatened or endangered, gather in places with similar elevations as they seek water of optimal depth for foraging on underwater vegetation (Liu and Ye, 2000). The aforementioned sub-lakes and large delta floodplains on the west side of the lake, formed by the sediments of the Ganjiang and Fuhe rivers, are especially important habitats. Ning et al. (2003) found that the *Oncomelania* snails that play host to *schistosome japonium*, which is the cause of the disease *schistosomiasis* and is endemic in the PLR, are always located on shoals inundated for about 113–216 days a year.

During the past several decades, the hydrological environment in the PLR has been modified greatly. Although land reclamation from the lake began in the Song dynasty (Council of Poyang, 1988; Wu, 1997), many of the current levees around Poyang Lake were built during the 1950s and 1960s (Table 1). Under the national government's "Grain First" policy, which was established in the mid-1950s and placed a high priority on grain production, farmlands were reclaimed from the lake

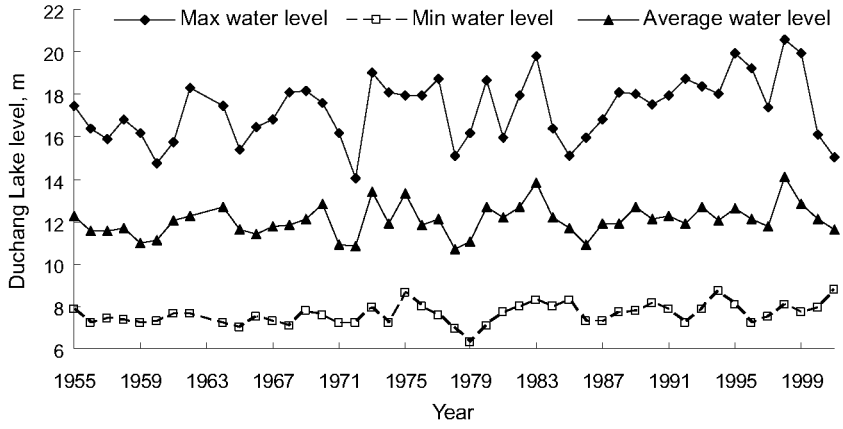

Fig. 2. Annual maximum, minimum, and average lake levels at the Duchang gauging station.

Table 1. Land Reclamation in the Poyang Lake Region since 1954

Survey year	1954	1957	1961	1965	1967	1976	1984	1995
Poyang Lake area (km^2)	5160	5004	4720	4410	4120	3914	3889	3859
Reclaimed area (km^2)	156	284	310	290	206	25	30	
Total reclaimed area since 1954 (km^2)	0	156	440	750	1040	1246	1271	1301

Source: Min, 1998.

area and the floodplain was enclosed into many polders that supported high population densities of about 400–800 persons/km^2 (Shankman et al., 2006). It is estimated that there were about 565 levees around Poyang Lake in 1998 (Min, 1998), and more than 330 levees were created during the 1950s and 1960s. As a result of reclamation of land from the lake, the free surface of Poyang Lake was reduced from an estimated area of 8,932 km^2 to 3,850 km^2 (Yu and Dou, 1999; Jiang, 2006). These levees were charged with protecting about 5,082 km^2 of farmland and settlements, and a population of about 10 million people (Peng, 1999). Most of the empoldered region has elevations in the range from 13 to 16 m.

A second major hydrological change was deforestation, which occurred in the drainage basin of the lake on a large scale during the 1950s to support the development of the steel industry. This deforestation resulted in increased runoff and erosion of sediments that were carried to Poyang Lake, and which also caused reduction in its storage capacity. As a result of sedimentation, Min (1999) estimated that the storage capacity of Poyang Lake was reduced by 4.8 percent from 1954 to 1997.

Finally, a number of large hydrological projects have been built in the Poyang Lake watershed. The Wan'an reservoir (created in 1993 along the middle reach of the

Ganjiang River), and the Zhelin reservoir (created in 1975 at the upper reach of the Xiushui River) provide for storage of floodwaters within the basin. Both of these reservoirs have reduced sediment delivery to the lake. The Three Gorges Dam is on the Yangtze River about 700 km upstream from the outlet of Poyang Lake. One study has argued that this new dam will intensify floods and droughts in the Poyang Lake floodplain (Liu and Wu, 1999). Shankman and Liang (2003) argued that, by discharging water from behind Three Gorges Dam so that the reservoir has flood storage capacity in July and August (when the upper basin tends to peak), higher water levels in the Yangtze River in May and June will meet the traditional flood peaks from the Poyang Lake basin and slow Poyang Lake's discharge to the Yangtze River. Reverse flow from the Yangtze River to Poyang Lake is a common phenomenon, but by peaking earlier Yangtze River flow could back up into the lake just as its own discharge is at its highest. Such a scenario would result in increased flood risk around the lake.

These three factors (wetland reclamation for agriculture, deforestation, and hydrologic projects) help explain the increase in annual maximum lake levels during 1955–2001 (Fig. 2). During this period, nine extreme (>18.9 m) floods occurred, in 1973, 1977, 1980, 1983, 1992, 1995, 1996, 1998, and 1999. The historical high lake level occurred during the 1998 flood, when the lake level at Duchang reached 20.6 m and exceeded the previous highest lake level (in 1995) by 0.64 m. It is estimated that more than 240 levees in the PLR were damaged in 1998 and more than 722 km^2 farmland was flooded (Jiang, 2006). As the reclaimed land on the Poyang floodplain flooded, more than 4 million households were damaged and more than 1.59 million people were left homeless (UN-Habitat, 2002).

In this study, by creating the WL-DEM and flood frequency maps, we attempt to provide a basis for our future work on flood risk analysis and bird habitat modeling that seeks to characterize and assess vulnerability of human and wildlife around Poyang Lake. The next section describes the data we used in this study.

DATA

DEM Data

We acquired a DEM for the PLR that had a spatial resolution of 30 m and that had been interpolated from elevation contours digitized from a map with a scale of 1:50,000. The contour interval was 5 m at low elevations and 10 m at higher elevations. We used the DEM both to map inundated extent according to lake level and for orthorectification of remote sensing images. The minimum recorded elevation in the DEM was 12 m, while the lowest observed elevation for Poyang Lake was about 5 m; so the DEM is only suitable for identification of inundated areas when lake levels are higher than 12 m amsl.

In addition, the SRTM DEM with 3 arc-second (~90 m) spatial resolution was acquired from USGS EROS Data Center (http://edc.usgs.gov/srtm/data/seamlesshelp.html). Because random phase noise is a well-known property of SRTM data (Walker et al., 2007), we first conducted phase noise removal by averaging the elevation values in a 3 × 3–pixel window. Overlaying the SRTM data on Landsat TM/ETM+ images and the contour-based DEM revealed a systematic horizontal offset between them. The SRTM data were shifted westward 3 pixels (270 meters) to align

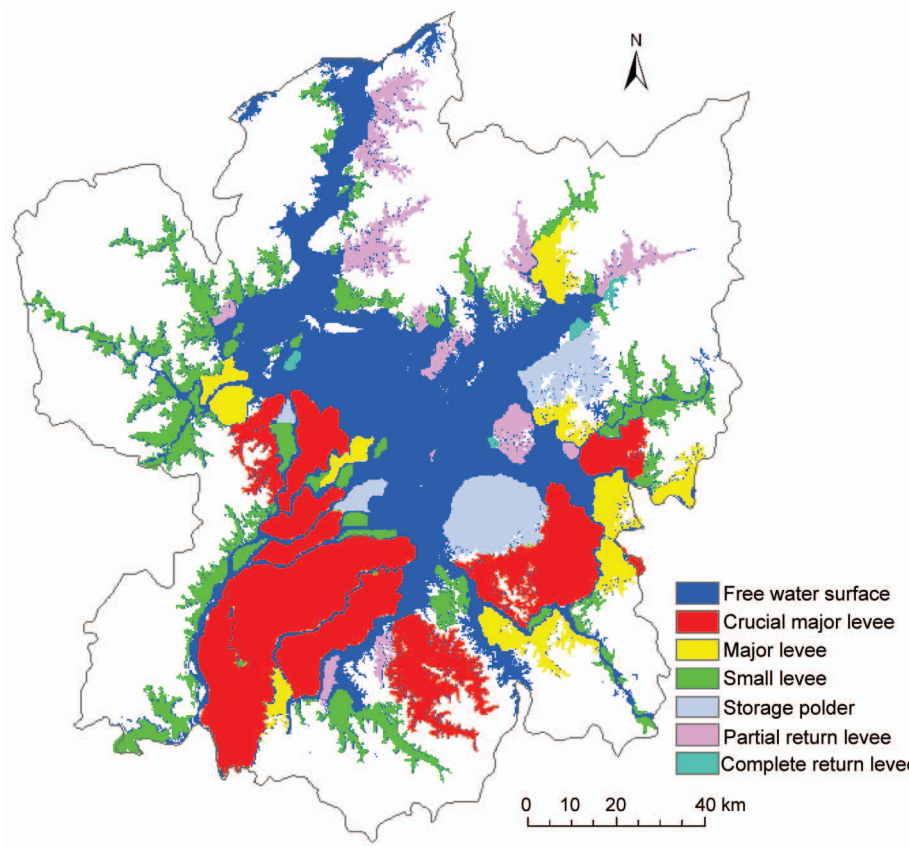

Fig. 3. Polders bounded by different types of levees.

them with the other data. The vertical datum for the SRTM DEM was the EGM 96 geoid. Because we had no direct way to convert from EGM 96 geoid to NVDC 1985, a flat area (15.25 km × 15.25 km) with little vegetation was selected to estimate a constant offset for the two vertical datums. We found that the SRTM DEM was 1 meter higher than the contour-based DEM on average and adjusted the SRTM data by subtracting 1 meter. Finally, the SRTM data were resampled to 30 m spatial resolution using nearest neighbor resampling so that it could be quantitatively compared with the contour-based DEM and the Landsat images. The lowest recorded elevation on the lake in the SRTM DEM was 9 meters. All DEM and image data were reprojected into UTM Zone 50N with WGS84 datum.

Levee Data

The levees around Poyang Lake were created to enclose the low-elevation floodplain for use as farmland, aquaculture, and settlements. These levees, with an average width of about 2~9 m, were classified and mapped (Fig. 3), based on interpretation of

Landsat TM/ETM+ imagery together with additional information from published sources (Jiangxi Province, 1999) and field surveys (Jiang, 2006).

Although the levees around the lake are charged with the protection of more than 5,000 km^2 of farmland and about 10 million people, most of them are not adequate for this purpose. Despite being designed for 100-year floods, the current condition of the 15 most important levees is such that they can only withstand floods with a recurrence interval of 5–8 years (Liu and Xu, 2004). Most of the levees were damaged to some extent, but did not collapse, during flood events in 1992, 1995, 1996, 1998, and 1999 (Liu and Xu, 2004).

The PLR levees have been categorized as crucial major levees, major levees, and minor levees according to the amount of enclosed farmland and settlement area. Crucial major levees enclose more than 66.7 km^2 farmland, plus big cities or capitals of counties and are designed to be sufficiently high and hard (i.e., concrete) to withstand floods with a 100-year recurrence interval. The major levees are also designed to defend against 100-year floods and are charged with protection of more than 33.3 km^2 farmland. There is less than 33.3 km^2 farmland behind the minor levees, and their polders are more vulnerable to flooding.

To improve the floodwater storage capacity of the lake, four major levees (Huanghu levee, Zhuhu levee, Kangshan dike, and Fangzhouxietang levee) were assigned to floodwater storage by the government of Jiangxi Province in 1986. According to the policy, the storage levees should be breached to allow floodwater to discharge when lake levels at Hukou (near the lake's outlet) reach 18.7 m, although they were not breached during the 1998 flood event because many minor levees and a major levee were destroyed by the flood (Shankman and Liang, 2003).

After the 1998 flood event, the government carried out a policy of "Returning Farmland to the Lake," and many minor polders were abandoned and farmland was converted back to wetland. The abandoned levees are classified as "partial return" and "complete return." In the "partial return" polders, villagers were resettled to higher ground, but the farmland can still be cultivated. According to the regulation, when the lake level reaches 18.7 m, partial return levees with protected areas less than 6.67 km^2 will be breached. When lake levels reach 19.8 m, the partial return levees with protected areas more than 6.67 km^2 will be breached. In the "complete return" polders, the villagers were resettled and the farmland was abandoned to wetland.

Lake-Level Records

Daily lake levels from seven hydrological stations (Duchang, Xingzi, Wucheng [Ganjiang], Wucheng [Xiushui], Tangyin, Kangshan, and Hukou) around Poyang Lake (Fig. 1) were obtained from the Hydrological Bureau of Jiangxi Province. The Wucheng station is at the intersection of Ganjiang River and Xiushui River and there are two gauges that are charged with monitoring these two rivers, respectively. Daily lake-level records were available for 46 years from 1955 to 2001 at each gauging station. The published lake-level records for these different stations were based on different elevation datums and were converted to the NVDC 1985 before further analysis.

Table 2. Dates of TM/ETM+ Images and Uses in the Current Study

Date for images taken	Uses in this study[a]
Dec. 17, 1987	a, b
July 15, 1989	a, b, c
Jan. 31, 1993	a, b
July 10, 1993	a, b, c
April 4, 1999	a, b
Nov. 16, 1999	a
Dec. 10, 1999	a, b
April 16, 2000	a, d
July 5, 2000	a, b, c
August 22, 2000	a, b, c
Sept. 23, 2000	a
Oct. 9, 2000	a, c, d
Jan. 29, 2001	a, b

[a]a = evaluate gauging stations; b = create digital water body model and flood-risk map; c = validate the DEM-based inundated extent model; d = validate the DWM-based inundated-extent model.

METHODS

Image Processing

Thirteen Landsat TM/ETM+ images that cover Poyang Lake (path 121/row 40) were acquired and put to several uses in this study (Table 2). Different subsets of these images were used to: (a) select a representative gauging station by relating remotely sensed inundated area with lake levels; (b) create a WL-DEM and flood frequency maps; (c) validate the DEM-based inundated extent models by comparing the DEM-based and remotely sensed inundation extents; and (d) validate the WL-DEM–based inundated-extent model by comparing the WL-DEM–based and remotely sensed inundation extent.

All images were orthorectified using the contour-based DEM. Although Landsat TM near-infrared (NIR) band 4 (0.76–0.90 μm) can usually discriminate water from land surface because of the low reflectance from water, water can be confused with asphalt in urban areas, which also has low reflectance in NIR. Wang et al. (2002) delineated water successfully by combining TM band 4 and TM band 7 (2.08–2.35 μm). However, Poyang Lake at high lake level is an expansive water body that exhibits enough spectral variation because of differences in sediment concentrations, flood depths, wetland plants, and discharge from factories and cities to confuse any single TM band or pair of bands. We delineated inundated extent using unsupervised classi-

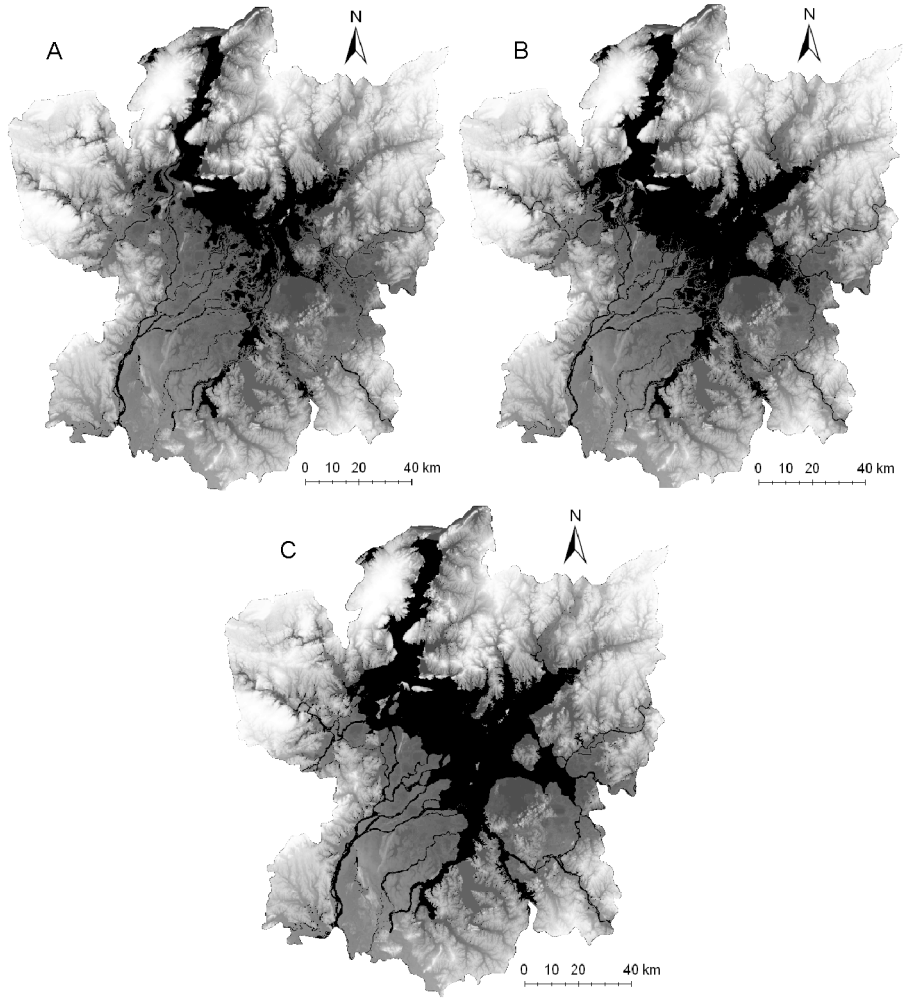

Fig. 4. Remotely sensed inundation extents (in black) from three example images—A. April 16, 2000; B. October 9, 2000; C. July 10, 1993—overlaid on a digital elevation model.

fication with all six 30 m spatial resolution bands as input. We used the ISODATA algorithm and identified 15 spectral classes in the images (Ridler and Calvard, 1978). Because Poyang Lake water exhibits spectral variability, water was included in several different spectral classes. All spectral classes referring to water, identified through visual interpretation of a pseudo-color image composite with TM7, TM4, and TM3 were combined to produce binary land-water images for each date (Fig. 4).

Characterizing Lake-Level Dynamics

In order to develop statistical descriptions of lake-level dynamics in the PLR, we selected a single gauging station to represent the dynamics of the entire lake. Logarithmic functions were fitted to the relationships between lake levels measured at each

station and the remotely sensed inundated areas (km^2) using ordinary least-squares regression, both including and excluding water that was enclosed by levees and, therefore, disconnected from the main lake. The gauging station with the best-fitting function was selected as the most representative and used in all subsequent modeling. In order to assess how well this single station represented the lake levels across the entire lake, we measured the differences between lake levels at the selected gauging station and those measured at the other stations for all available days.

We used the records from the representative gauging station to calculate exceedance probabilities (EPs). Because the configuration of Poyang Lake was modified by reclamation during the 1950s and 1960s (Table 1), only the lake levels recorded during 1970–2001 were used to calculate EPs for all lake levels. The EPs for all lake levels measured on the dates of nine of the TM/ETM+ images (Table 2) were then assigned to the boundaries derived from those images. We did not use additional images because they either represented redundant information in terms of lake levels or, in two cases, they were set aside for evaluating the accuracy of the WL-DEM. A flood frequency map was then created using spline interpolation based on the 10 contour lines, including the waterline of the modeled maximum inundation extent at a 20.6 m lake level in a 1998 flood (ESRI, 2006).

WL-DEM

Because of the 5 m contour interval in the contour-based DEM and the relatively coarse resolution of the SRTM DEM (90 m), we expected difficulties in characterizing the inundation extents when the lake was at low levels. To improve our ability to model medium and low lake levels, we supplemented these DEMs with data from the Landsat images. Assuming that inundation extent is only a function of lake level measured at the representative gauging station, the boundaries of inundation extents from the nine TM/ETM+ images used to represent exceedance probabilities (above) were taken as isolines of lake level. The values of the isolines were assigned as the lake level measured at the representative gauging station on the day the image was obtained. The minimum and maximum lake levels for the imagery dates were 5.69 m (measured at Hukou on January 31, 1993) and 18.43 m (measured at Tangyin on July 10, 1993), respectively (Table 3). The WL-DEM was created by spline interpolation using ArcGIS with the boundaries of remotely sensed inundation extents. To complete the WL-DEM, we supplemented it with elevation values from the contour-based DEM for the regions that were (a) higher than 18.36 m or (b) enclosed by levees.

Evaluating Inundation-Extent Models

Assuming that all areas with elevations lower than the lake level measured at the representative gauging station are inundated, we modeled the inundation extent using the contour-based DEM, SRTM DEM, and WL-DEM. The Kappa coefficient (Cohen, 1960) was used to evaluate the agreement between modeled and remotely sensed inundation extents. The Kappa coefficient reflects the proportion of cells that agree on the classification as inundated or not, after chance agreement is removed. We refer to the general benchmarks for interpreting Kappa suggested by Landis and Koch (1977), where 0.41–0.60, 0.61–0.80, and 0.81–1.00 can be interpreted as indicating moderate

Table 3. Lake Levels Measured at Seven Hydrological Stations and Remotely Sensed Inundation Areas for each Landsat Image Date

Lake level, in m: Date	Xingzi	Wucheng (Xiushui)	Wucheng (Ganjiang)	Tangyin	Kangshan	Duchang	Hukou	Inundated area (km^2)[a]	Inundated area (km^2)[b]
Dec. 17, 1987	8.28	10.04	10.16	10.90	12.05	9.73	7.51	1489.4	2613.9
July 15, 1989	17.36	17.35	17.35	17.42	17.27	17.35	17.56	3330.9	4925.8
Jan. 31, 1993	6.65	9.08	9.21	10.01	11.11	8.32	5.69	986.6	1866.2
July 10, 1993	18.29	18.32	18.33	18.43	18.32	18.36	18.26	3522.4	6530.4
April 6, 1999	10.18	11.43	11.55	12.34	13.13	11.48	7.35	2081.7	3354.7
Nov. 16, 1999	11.02	11.38	11.39	11.53	12.02	11.27	10.96	1933.2	3250.4
Dec. 10, 1999	8.72	9.81	9.74	10.29	11.46	9.29	8.61	1312.9	2642.9
April 16, 2000	10.45	11.77	10.72	11.97	12.95	11.23	9.92	2090.5	3080.5
July 5, 2000	15.54	15.52	15.55	15.59	15.45	15.54	15.68	3152.4	4281.0
Aug. 22, 2000	13.73	13.83	13.81	13.82	13.72	13.72	13.85	2668.2	4159.7
Sept. 23, 2000	14.13	14.17	14.16	14.25	14.11	14.16	14.23	3197.3	4788.0
Oct. 9, 2000	14.14	14.15	14.13	13.22	13.24	14.13	14.28	3001.1	4336.9
Jan. 29, 2001	8.72	11.35	11.43	12.04	13.09	11.03	8.49	2111.6	3957.1

[a]Excluding area enclosed by levee.

[b]Including area enclosed by levee.

agreement, substantial agreement, and almost perfect agreement, respectively. Because we are performing many comparisons with varying population sizes (i.e., number of pixels; described below), we did not attempt to perform significance tests, but rather use Kappa as an indicator of relative strength of agreement among the different models.

A complicating factor in this analysis is that the accuracies are spatially heterogeneous, i.e., regions far away from the boundary of the water body will have higher accuracies than regions near the boundary. To characterize this heterogeneity and better understand the strength of agreement, buffers with distances of 1,2,…,10 pixels were created from the remotely sensed water boundary and the Kappa coefficient was used to evaluate the accuracy of the modeled water body in each of these buffers (i.e., all pixels within the specified distance were included in the Kappa calculation). We report Kappa as a function of buffer distance from the observed water boundary. Because the pixels nearest to the water boundary are those most likely to be misclassified by the model, the error rate should increase (and the accuracy decrease) as the analysis focuses on those pixels (i.e., as the buffer distance decreases). For flood-risk mapping in land use management and emergency response, measuring accuracy over the narrowest distance buffers imposes a standard that is too high; rather understanding the general patterns of inundation (e.g., averaged over larger areas) is often sufficient. Therefore, considering the levels of agreement at larger distances should be sufficient. However, if flood-risk mapping is to be used for engineering purposes, accuracy standards should be higher and accuracy statistics should be interpreted at the narrowest distance bands. In any case, including all pixels in the region in the analysis (i.e., not using buffers to focus the analysis) imposes a standard that is too low, because all areas that are correctly identified as not inundated because they are nowhere near the water boundary are included in the analysis.

We compared the inundation extent modeled with each of the three DEMs with that observed on a number of Landsat images. We selected five images to represent a range from medium to high lake levels to test the DEM-based model (Table 2): August 22, 2000; October 9, 2000; July 5, 2000; July 15, 1989; and July 10, 1993. Because the water bodies enclosed by levees have no direct hydrological connection with Poyang Lake, we did not attempt to model inundation area behind the levees on the basis of lake levels and therefore compared inundation extents at places along the lake boundary with no levees present. The result is a conservative estimate of the accuracy of the inundation extent of the main lake, however, because inundation of areas bounded by levees can be mapped with a high degree of accuracy given information about the location and height of levees. We did not try to model the inundation extent for low lake levels because the contour-based and SRTM DEM data limit our ability to represent only those areas above 12 m and 9 m, respectively. The WL-DEM was created to improve our ability to model inundation areas at lower water levels, and was based on inclusion of water boundary contours from 10 images. We compared WL-DEM–based inundation extents with extents observed in two scenes that were not used in the creation of the WL-DEM and that represented medium and low lake levels.

RESULTS AND DISCUSSION

Representative Gauging Station

The fit of the relationship between lake levels and inundated areas as measured from Landsat images (Fig. 5) was used as a measure of how representative each of seven hydrological stations was for modeling the entire lake (Table 3). The increase in inundated area with lake level was logarithmic in all cases, and the relationships based on inundated area that excluded inundated areas enclosed by levees fit better than those that included enclosed water for all but the Kangshan gauge. The water bodies behind levees are mainly natural or human-made ponds, and these water bodies have no direct hydrologic connection with Poyang Lake.

Among the seven gauging stations, the lake level from Duchang was best correlated with inundated area ($R^2 = 0.965$). Thus, we concluded that Duchang is the most representative station that can be as input to DEM-based models of inundated area within the area outside the levees. This result is in agreement with those of Min (2004). Duchang is located near the middle of the eastern lakeshore (Fig. 1). The lake levels from Duchang were used to drive subsequent inundation-extent models and flood frequency maps.

The median differences and variation in differences between Duchang lake levels and measurements made at the other six gauges during 1955–2001, which reflect the degree to which the Duchang measurements inaccurately represent the entire lake surface, decreased with increasing lake level (Fig. 6). The maximum difference was about 5 m at the lowest measured lake levels (~6 m). These results indicate that the Duchang station represents well the levels across the entire lake at levels above about 11 m, but that at levels of 11 m or less, there is substantial heterogeneity in the lake levels. This limits the ability of models based on lake levels measured at a single gauging station to appropriately represent the entire lake at low lake levels, but suggests that such models can be reasonably useful for representing lake dynamics at higher lake levels.

DEM-Based Models of Flood-Inundation Extent

The Kappa coefficients resulting from the comparison of contour-based (Fig. 7A) or SRTM-based (Fig. 7B) DEM inundation extents with the satellite classifications for the five test dates always increased as pixels at increasing distances from the observed water boundary were included in the calculation. This suggests that the suitability of inundation extent models for any given purpose will depend on the amount of spatial specificity required from the model. In all cases, the modeled inundated areas exhibited a substantial level of agreement (Kappa > 0.6) with image data, when observed over a 600 m band around the observed water boundary (i.e., 10 pixels on each side of the boundary). However, when observed over a 60 m band, there was not even moderate agreement in most cases. This indicates a non-homogeneous surface of the lake, i.e., the lake water level is dynamic and complicated.

For the models based on the DEMs, the Kappa coefficients corresponding to dates with higher lake levels (i.e., July 10, 1993 and July 15, 1989) were always

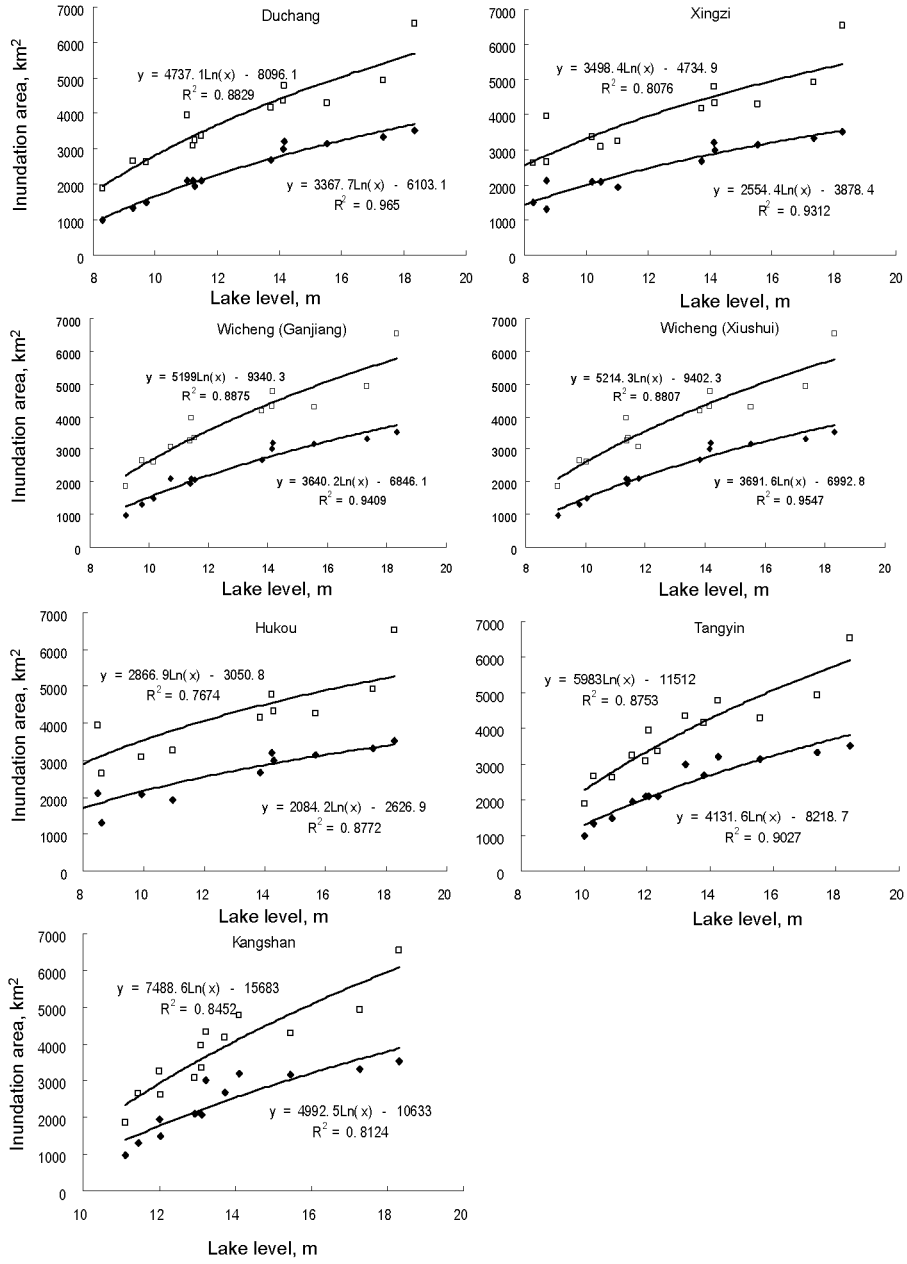

Fig. 5. Fitted relationships between remotely sensed inundation extents and lake levels for seven hydro-stations in Poyang Lake. Open squares represent data that include water enclosed by levees and solid diamonds exclude the water enclosed by levees.

higher than those for dates with lower lake levels (i.e., August 22, 2000 and October 9, 2000) at the same buffer distance. Although all dates included in this analysis had lake levels above 11 m, the general trend of increasing spatial heterogeneity of lake

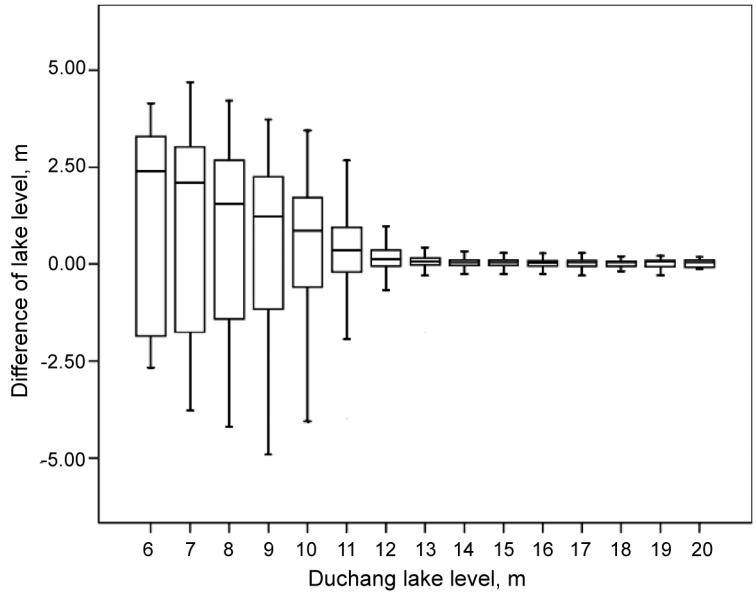

Fig. 6. Box plot of differences between measurements made at Duchang and the six other gauging stations for all days between 1955 and 2001.

levels at lower levels (Fig. 4) might still cause a violation of the assumption of constant lake levels and, therefore, explain the lower levels of agreement at medium and low lake levels. The increasing accuracy of the DEMs in representing inundation areas at high lake levels suggests that there is some promise in using such models for flood-risk mapping where the concern is with mapping risks associated with the highest lake levels, although the DEMs alone do not appear to provide sufficient detail for mapping inundation areas at low and medium lake levels.

The modeled inundation extents based on the SRTM DEM were always lower than those using the contour-based DEM, but the differences generally declined as more pixels were included in the calculation (i.e., at larger buffer distances) and at lower lake levels. Accuracies of inundated areas based on the SRTM DEM that were averaged over a distance of two or more pixels from the water boundary were roughly comparable to those from the contour-based DEM (Fig. 7). These results suggest that the SRTM-based DEM is not as good as the contour-DEM in providing a model of inundated area, but that the differences in accuracy were relatively small. This is at least partially related to differences in resolution, and it could be that the 30 m SRTM-based DEM, which was not available for our study, could be as good as or better than the contour-based DEM. Further analysis of the accuracy of the SRTM DEM for modeling flooding extent will be important for extending the type of analysis presented here to the broader geographic extent covered by the SRTM data.

Slope angle is likely to have some effect on the accuracy of inundation modeling at low lake levels based on DEM. As slope decreases, vertical error would naturally effect the horizontal position of the flood extent at an increasing rate (Hodgson and Bresnahan, 2004). However, we observed that the slope at the water boundary of

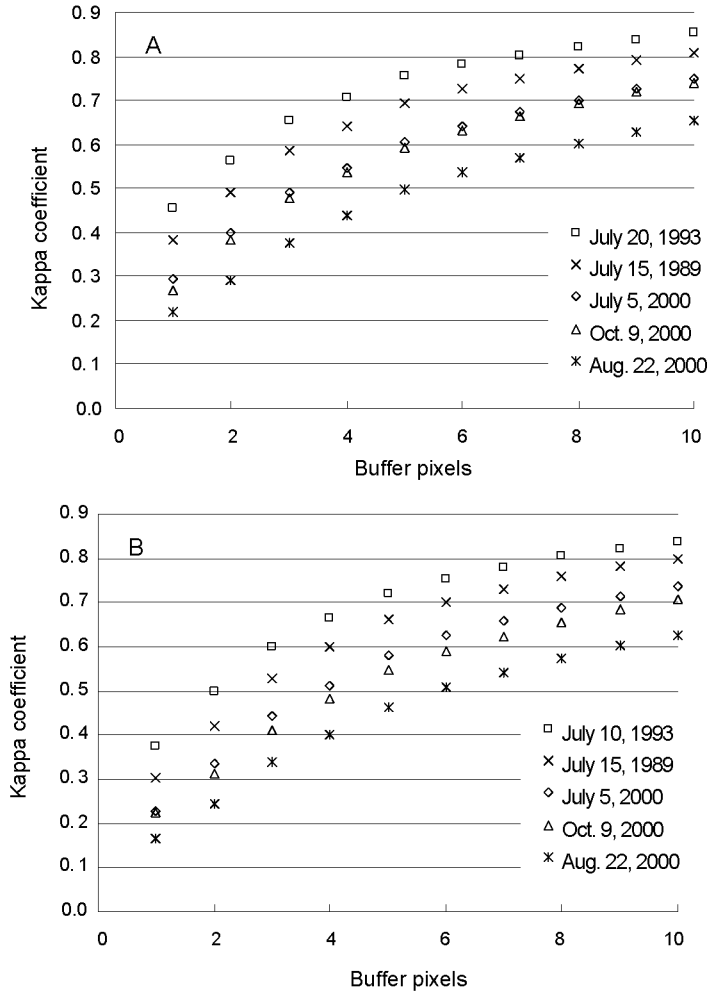

Fig. 7. Kappa coefficients for DEM-modeled inundation extents compared to Landsat images from five different dates. A. Contour-based DEM. B. SRTM. Distance buffers were defined relative to the remotely sensed water-body boundary.

flood extent is quite homogeneous. Pixels in the 10-pixel buffer had an average slope of 0.75°, with a standard difference of 0.021. Because of this relative homogeneity, variability in the slope in the Poyang Lake Region had a negligible effect on variability in the accuracy of the flooding extent models.

WL-DEM–Based Inundation Extent Modeling

Because the WL-DEM (Fig. 8) includes DEM elevations at higher elevations (above 18.36 m), the inundation extents based on the WL-DEM should be similar to those based on the DEM in high-water conditions, and we evaluated modeled inundation extents from the WL-DEM for only medium and low lake levels. Also, because

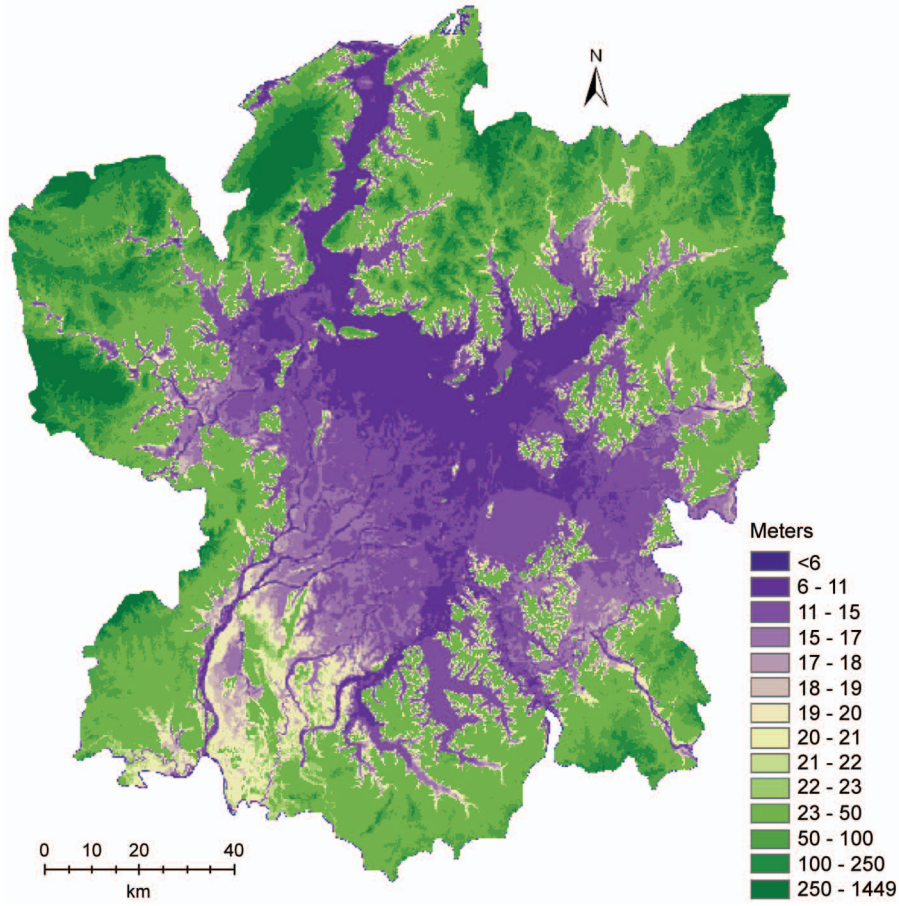

Fig. 8. The Water Line DEM for PLR.

the contour-based DEM produced better inundation estimates than the SRTM-DEM, only the inundation extents from the contour-based DEM were compared with WL-DEM–based inundation extents. Comparing the DEM-based and WL-DEM–based modeled inundation extents for one date (Fig. 9), it is clear that the WL-DEM–based inundation extent exhibits much more spatial detail near the mouths of the Ganjiang and Fuhe rivers than the DEM-based model. The comparison of Kappa coefficients for the contour-DEM–based and WL-DEM–based inundation extents also shows that the WL-DEM–based model is slightly better than the DEM-based model at medium lake levels (Fig. 10). The WL-DEM–based model had a moderate level of agreement with the remotely sensed inundation extent taken at a medium lake level, at distances greater than 60 m (i.e., 2 pixels) from the water boundary.

Because of the apparently low level of accuracy of the DEM-based inundation models at low lake levels, we did not compare the DEM-based and WL-DEM-based models for low lake levels. The WL-DEM–based inundation extent had a reasonable

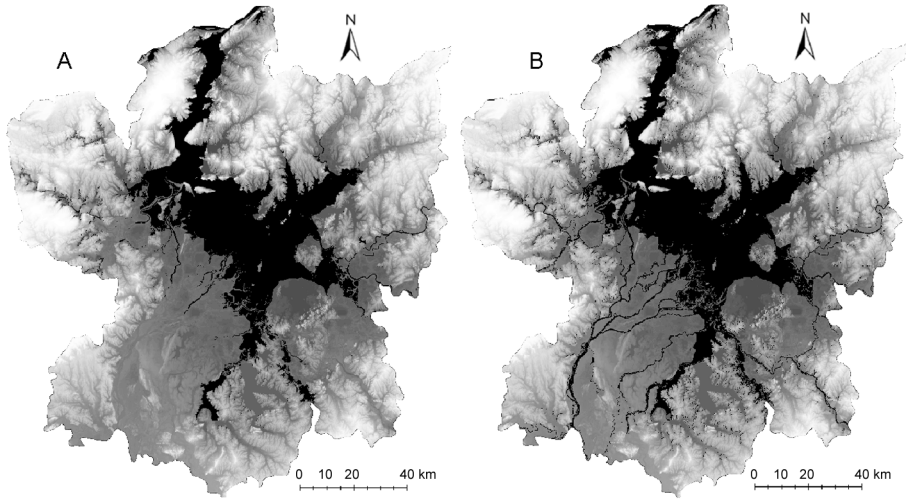

Fig. 9: The DEM-based (A) and DWM-based (B) modeled inundation extent for October 9, 2000 (Duchang level = 14.13 m).

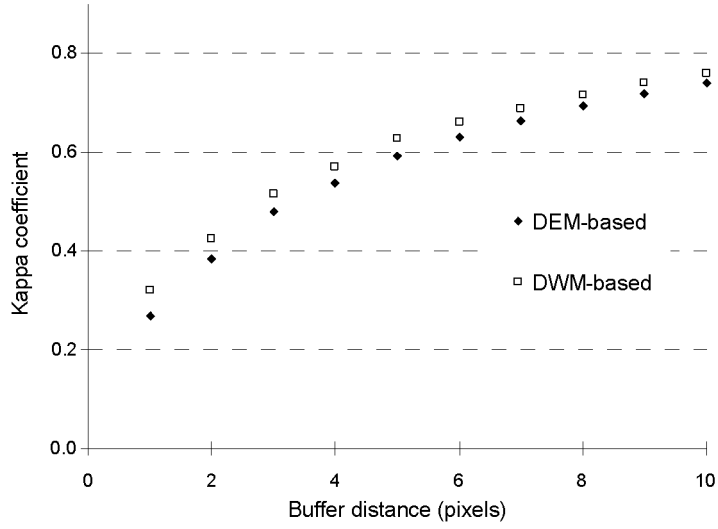

Fig. 10. Kappa coefficients for DEM-based and DWM-based inundation extents for October 9, 2000 within buffer distances from the remotely sensed water-body boundary.

amount of detail for the water body at the mouth of the river at a relatively low lake level (Fig. 11). The Kappa coefficient suggests that the WL-DEM was not able to accurately represent inundation extents at low lake levels (Fig. 12). The resulting inundation extent map had moderate levels of agreement with the remotely sensed

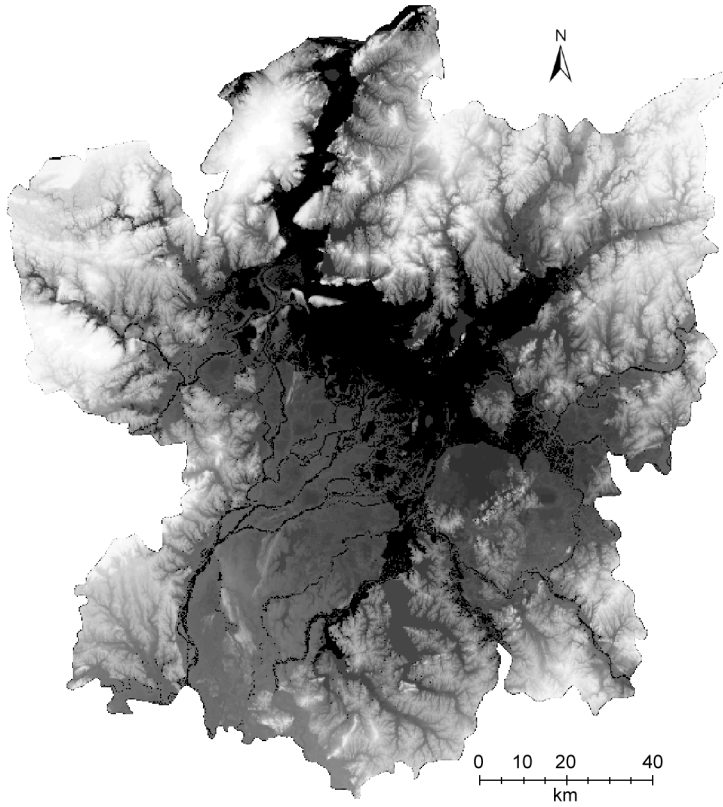

Fig 11. DWM-based modeled inundation extent for April 16, 2000 (Duchang level = 11.23 m).

data at distances greater than 120 m (i.e., four pixels) from the water boundary and reached a Kappa of 0.6 only at a buffer distance of 300 m (i.e., 10 pixels).

The presence of levees, along with the complex hydrology of the lake, complicates our ability to represent its dynamics with simple inundation models of this sort. Our analysis the agreement of inundation areas focused on parts of the lake boundary without levees present. A complete model of inundation must consider the constraints on flow imposed by the levee system. Furthermore, several smaller lakes around the boundary of Poyang Lake, such as Bang Lake, are hydrologically disconnected from the main lake. Hu et al (1997) has compared the lake level from Bang Lake and the Wucheng (Xiushui) hydrological station and found that the Bang Lake level does not track with the Wucheng (Xiushui) lake level when lake levels are low. For that reason there is a weak relationship between the Duchang lake level and the inundation area of the sub-lakes. For example, the water body of Bang Lake (Fig. 13) was wider on January 29, 2001 (lake level at Duchang was 11.03 m) than on April 6, 1999, when the Duchang Lake's level was higher (11.48 m). This is an important source of error in the WL-DEM–based inundation extent model for the sub-lakes, and limits its usefulness for modeling bird habitats around these sub-lakes.

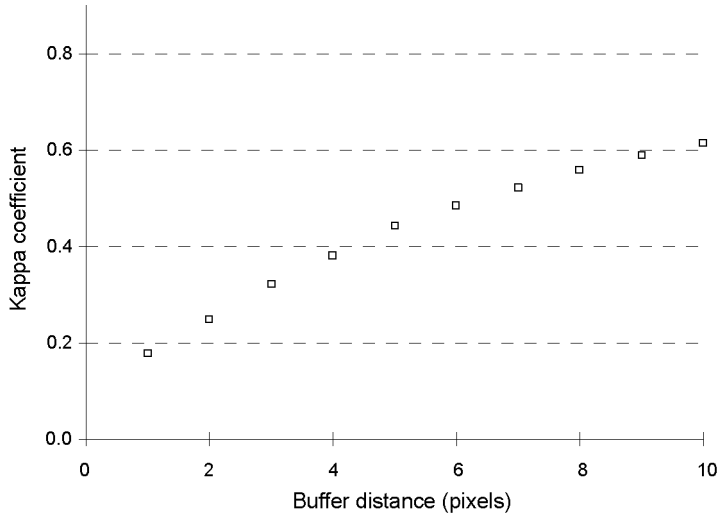

Fig. 12. Kappa coefficients for DWM-based inundation extents for April 16, 2000 (Duchang level = 11.23 m) within buffer distances from remotely sensed water-body boundary.

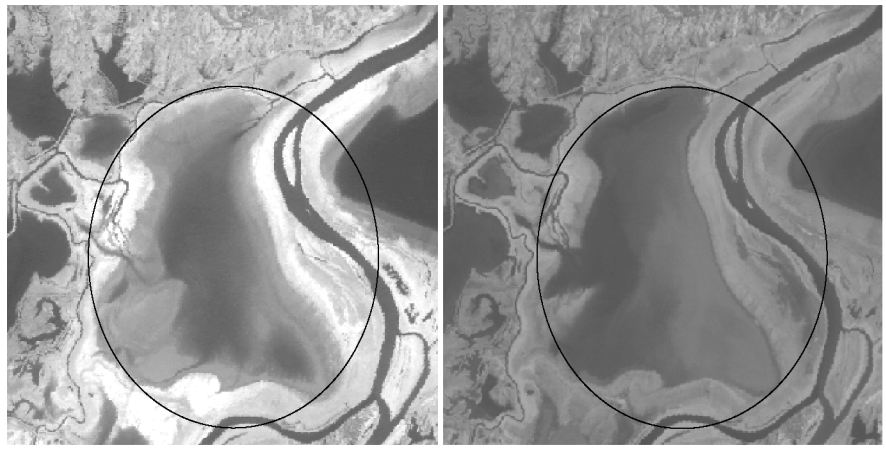

Fig. 13. An example of the inundation extent for a sub-lake (Bang Lake) of Poyang Lake.

Exceedance Probabilities and Flood Frequency Mapping

We calculated exceedance probabilities based on the daily lake-level records at Duchang from 1970 to 2001 and, because flooding events happen in June, July and August, separately for those months (Fig. 14). Taking the boundaries of remotely sensed inundation extents as EP isolines (based on Table 4), we mapped flood frequencies for annual, June, July, and August conditions (Fig. 15) within the boundary of modeled inundation extent for historic maximum lake level measured at Duchang

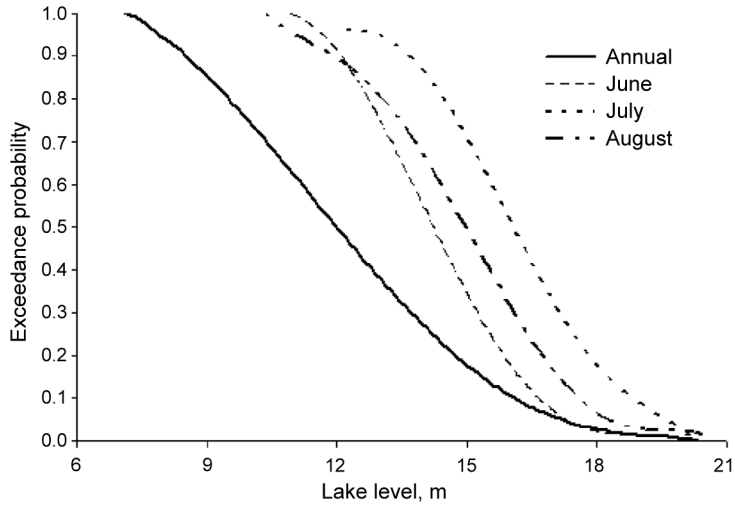

Fig. 14. The exceedance probabilities for every Duchang Lake level from 1970–2001 records, annually and for June, July, and August.

Table 4. Exceedance Probabilities for Lake Levels Associated with Landsat Image Dates

Image dates	Duchang lake level, m	EP yearly	EP in June	EP in July	EP in August
Dec. 17, 1987	9.73	0.774	1	1	1
July 15, 1989	17.35	0.045	0.054	0.274	0.021
Jan. 31, 1993	8.32	0.919	1	1	1
July 10, 1993	18.36	0.021	0.020	0.144	0.054
April 6, 1999	11.48	0.562	0.966	0.998	0.962
Dec. 10, 1999	9.29	0.816	1	1	1
July 5, 2000	15.54	0.137	0.260	0.605	0.398
Aug. 22, 2000	13.72	0.294	0.585	0.890	0.702
Jan. 29, 2001	11.03	0.623	0.988	1	0.972

(20.60 m). Because the lowest lake level of the permanent water body (6.28 m), which occurred on December 29, 1979, is below the minimum elevation in the DEM and because no remote sensing images were available on December 29, 1979, we were not able to distinguish the permanent water area with EP = 1 from the yearly flood frequency with EP = 0.919. This approach is useful, however, for the purposes of evaluating flood risk, because the minimum lake levels in June, July, and August are all greater than 8.32 m, so the monthly permanent water body can be mapped for the flood season.

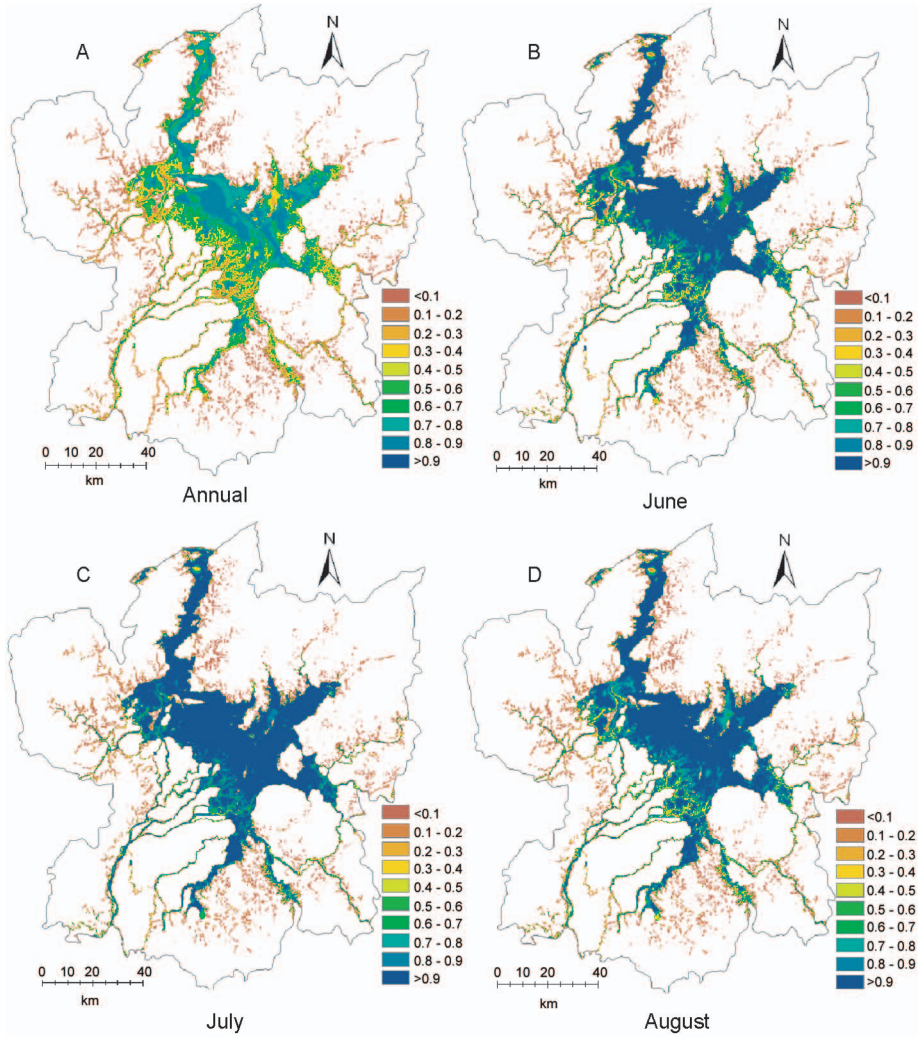

Fig. 15. The Annual (A), June (B), July (C), and August (D) inundation probability for the Poyang Lake region.

CONCLUSIONS

Thirteen Landsat TM/ETM+ images were used to identify the inundated area in and around Poyang Lake. These areas were regressed against measured lake levels from seven hydrological stations in Poyang Lake. From the correlation coefficients, we concluded that the Duchang station was the most representative hydrological station for evaluating inundation extent.

Based on lake levels measured at Duchang, we used two approaches for mapping the inundation extent for Poyang Lake floodplain and compared their results with the remotely sensed inundation extents as reference. Because the lake levels are more

variable as lake level decreases, the inundation extent from the DEM-based model is most reasonable for high lake level conditions, but is not suitable for representing inundation extent at medium and low lake levels. The results of inundation modeling using the SRTM DEM were not as good as the contour-based DEM for the floodplain area, but the SRTM DEM may be a reasonable substitute where other sources are unavailable. Because we did not have access to the 30 m resolution SRTM DEM, we can only speculate that some of the difference in accuracy is due to the coarser resolution of the SRTM DEM.

Using the boundaries of remotely sensed inundation extents as isolines of lake level, a digital water-level model (WL-DEM) was created for modeling inundation extent at medium and low lake levels. The WL-DEM–based inundation extents were better than the DEM-based models at both low and medium lake levels. These results point to an important advantage of combining digital elevation data with remotely sensed images of inundation in representing flood dynamics, and suggest the possibility of using such data to improve habitat characterizations at low lake levels. Information on lake levels, combined with the WL-DEM and a map of levees with heights, can therefore do a reasonably good job of representing flood inundation around Poyang Lake when lake levels are high and where levees are not present (i.e., where we evaluated accuracy). This is useful because flood-risk assessments are generally concerned with high, rather than low, lake levels. When lake levels are low, the inundation extent in the sub-lakes cannot be improved by using WL-DEM, because of the hydrological disconnection between the sub-lakes and the main lake at low lake levels. The WL-DEM provides additional details in the main lake at low lake levels and increases the inundation-extent model accuracy at medium lake levels. Because the habitats for most waterbirds are below 18 meters (Liu, 2000), the WL-DEM is useful for bird habitat modeling. However, habitat for wetland birds that over-winter in the region when lake levels are low are very sensitive to variations in lake level. Future work should build on more extensive archives of satellite data from multiple platforms to build more complete representations of the flood dynamics in the Poyang Lake Region (Andreoli et al., 2007) and elsewhere. To help bird habitat modeling around sub-lakes, separate hydrological gauging stations are required to accurately represent lake levels and inundation areas within these sub-lakes.

The annual and flood-season monthly flood frequencies were mapped by using the remotely sensed inundation extents as isolines and assigning them with lake-level exceedance probability estimated from Duchang data. These flood frequency maps will be used as important inputs to integrated assessment of flood dynamics, ecological processes, and human vulnerabilities, and can be used in planning, design, and management of flood works, natural reserves, and land use and land cover policies.

ACKNOWLEDGMENTS

We acknowledge financial support for this project from the U.S. National Aeronautics and Space Administration (NASA; Grant No. NEWS/04-1-0000-0025), the U.S. National Science Foundation (NSF; Grant No. BCS-0527318), and the National Science Foundation of China (NSFC; Grant No. 40561011). We also wish to thank Shuming Bao, Lin Zheng, and Ying Liu for their collaboration and for arranging logistical support in the field.

REFERENCES

Andreoli, R., Yesou, H., Li, J., and Y. Desnos, 2007, "Synergy of Low and Medium Resolution ENVISAT ASAR and Optical Data for Lake Watershed Monitoring: Case Study of Poyang Lake (Jiangxi, P.R. China)," paper presented at ENVISAT Symposium 2007, Montreaux, Switzerland, April 2007.

Bhavsar, P., 1984, "Review of Remote Sensing Applications in Hydrology and Water Sources Management in India," *Advances in Space Research*, 4(11):193–200.

Cohen, J, 1960, "A Coefficient of Agreement of Nominal Scales," *Educational and Psychological Measurement*, 20:37–46.

Council of Poyang Lake Research Editors, 1988, *Researches on Poyang Lake*, Shanghai, China: Shanghai Science & Technology Press, 118 p. (in Chinese).

Correia, F. N., Rego, F. C., Saraiva, M. D. S., and I. Ramos, 1998, "Coupling GIS with Hydrologic and Hydraulic Flood Modeling," *Water Resources Management*, 12:229–249.

Deutsch, M., Ruggles, F., Guss, P., and E. Yost, 1973, "Mapping the 1973 Mississippi Floods from the Earth Resource Technology Satellites," in: *Proceedings of the International Symposium on Remote Rensing and Water Resource Management*, Burlington, Canada: American Water Resource Association, No. 17, 39–55.

ESRI, 2006, *ArcGIS v. 9.2.*, Redlands, CA: Environmental Systems Research Institute.

Gianinetto, M., Villa, P., and G. Lechi, 2006, "Postflood Damage Evaluation Using Landsat TM and ETM+ Data Integrated with DEM," *IEEE Transactions on Geoscience and Remote Sensing*, 44(1):236–243.

Hodgson, M. E. and P. Bresnahan, 2004, "Accuracy of Airborne Lidar Derived Elevation: Empirical Assessment and Error Budget," *Photogrammetric Engineering and Remote Sensing*, 70(3):331–339.

Hu, C. H., Jiang, J. H., and H. H. Zhu, 1997, "Analysis on Water-Level Relationships between Banghu Depression and Poyang Lake and Its Submission and Emersion of Bottomland," *Oceanology et Limnology Sinica*, 28(6):617–623 (in Chinese).

Hunter, G. J. and M. F. Goodchild, 1995, "Dealing with Error in Spatial Databases: A Simple Case Study," *Photogrammetric Engineering and Remote Sensing*, 61(5):529–537.

Islam, M. D. M., and K. Sado, 2000, "Development of Flood Hazard Maps of Bangladesh Using NOAA-AVHRR Images with GIS," *Hydrological Sciences Journal*, 45(3):337–355.

Jiang, L. 2006, "Flood Risk and Land Use Change in the Wetland Restoration Area Around Poyang Lake, China," Ph.D. dissertation, Institute of Geographical Science and Natural Resources Research, Chinese Academy of Sciences, Beijing, China (in Chinese).

Jiangxi Province Department of Water Resources, 1999, *Levee Atlas of Jiangxi Province*, Nanchang, China: Jiangxi Province Department of Water Resources (in Chinese).

Kim, D. J., Moon, W. M., Park, S. E. Kim, J.-E., and H. S. Lee, 2007, "Dependence of Waterline Mapping on Radar Frequency Used for SAR Images in Intertidal Areas," *IEEE Geoscience and Remote Sensing Letters*, 4(2):269–273.

Landis, J. R. and G. G. Koch, 1977, "The Measurement of Observed Agreement for Categorical Data," *Biometrics,* 33:159–173.

Lee, J., Snyder P. K., and P. F. Fisher, 1992, "Modeling the Effect of Data Errors on Feature Extraction from Digital Elevation Models," *Photogrammetric Engineering and Remote Sensing*, 58:1461–1467.

Liu, R. and C. Xu, 2004, "The Anti-2 Seepage Design and Analysis of the Levee Body of Liuhu Dike on the Second Stage Flood Control Project of Poyang Lake," *Jiangxi Hydraulic Science & Technology*, 30: 54–60 (in Chinese).

Liu, X. and D. Wu, 1999, "Brief Analysis of the Effect of the Poyang Lake Water Level in Flood Period by the Three-Gorges Project," *Jiangxi Hydraulic Science and Technology*, 25(2):71–75 (in Chinese).

Liu, X. Z. and J. X. Ye, 2000, *The Jiangxi Wetland*, Beijing, China: China Forest Publishing Company (in Chinese).

Min, Q., 1998, "Analysis on the Influence of Reclamation on Flood in Poyang Lake Region," *Jiangxi Hydraulic Science & Technology*, 24(3):177–185 (in Chinese).

Min, Q., 1999, "Evaluation of the Effects of Poyang Lake Reclamation on Floods," *Yangtze River*, 30(7): 30–32 (in Chinese).

Min, Q., 2004, "Analysis and Calculation of Frequency Variation of Flood Stages in Poyang Lake," *Hydrology*, 24(4): 17–20.

Niedermeier, A., Hoja, D., and S. Lehner, 2005, "Topography and Morphodynamics in the German Bight Using SAR and Optical Remote Sensing Data," *Ocean Dynamics*, 55(2):100–109.

Ning, A., Chen, N. G., Zhong, J. H., Chen, H. G., Lin, D. D., Liu, H. Y., Gao, Z. L., Liu, Y. M., Hu, F., and S. J. Zhang, 2003, "Study of the Relationship Between Snail Distribution of Marshland and Changes of Water Level in Poyang Lake Region," *China Journal of Schistomiasis Control*, 15(6):429–433 (in Chinese).

Peng, D. Z., Xiong, L. H., Guo, S. L., and N. Shu, 2005, "Study of Dongting Lake Area Variation and Its Influence on Water Level Using MODIS Data," *Hydrological Sciences Journal*, 50(1):31–44.

Plate, E. J., 2002, "Flood Risk and Flood Management," *Journal of Hydrology*, 267:2–11.

Rabus, B., Eineder, M., Roth, A., and R. Bamler, 2003, "The Shuttle Radar Topography Mission—A New Class of Digital Elevation Models Acquired by Spaceborne Radar," *ISPRS Journal of Photogrammetry and Remote Sensing*, 57(4):241–262.

Rango, A. and V. V. Solomonson, 1974, "Regional Flood Mapping from Space," *Water Resource Research,* 10(3):473–484.

Ridler, T. W. and S. Calvard, 1978, "Picture Thresholding Using an Interactive Selection Method," *IEEE Transactions on Systems, Man, and Cybernetics*, Smc-8(8):1264–1291.

Sanders, B. F., 2007, "Evaluation of On-line Dems for Flood Inundation Modeling," *Advances in Water Resources*, 30(8):1831–1843.

Sanyal, J., and X. X. Lu, 2005, "Remote Sensing and GIS-Based Flood Vulnerability Assessment of Human Settlements: A Case Study of Gangetic West Bengal, India," *Hydrological Processes*, 19(18): 3699–3716.

Sanyal, J., and X. X. Lu, 2004, "Application of Remote Sensing in Flood Management with Special Reference to Monsoon Asia: A Review," *Natural Hazards*, 33(2):283–301.

Shankman, D., Keim, B. D., and J. Song, 2006, "Flood Frequency in China's Poyang Lake Region: Trends and Teleconnections," *International Journal of Climatology*, 26:1255–1266.

Shankman, D. and Q. Liang, 2003, "Landscape Changes and Increasing Flood Frequency in China's Poyang Lake Region," *Professional Geographer*, 55(4):434–445.

Smith, R. K. and K. R. Bryan, 2007, "Monitoring Beach Face Volume with a Combination of Intermittent Profiling and Video Imagery," *Journal of Coastal Research*, 23(4):892–898.

Townsend P. A. and S. J. Walsh, 1998, "Modeling Floodplain Inundation Using an Integrated GIS with Radar and Optical Remote Sensing," *Geomorphology*, 21:295–312.

UN-Habitat, 2002, "Best Practice—Post-flood Resettlement in the Poyang Lake Region," Jiangxi Province Together Foundation and UN-Habitat [http://database.bestpractices.org/bp_display_best_practice.php?best_practice_id=61].

Wang, Y., Colby, J. D., and K. A. Mulcahy, 2002, "An Efficient Method for Mapping Flood Extent in a Coastal Floodplain Using Landsat TM and DEM Data," *International Journal of Remote Sensing*, 23(18):3681–3696.

Walker, W. S., Kellndorfer, J. M.., and L. E. Pierce, 2007, "Quality Assessment of SRTM C- and X-band Interferometric Data: Implications for the Retrieval of Vegetation Canopy Height," *Remote Sensing of Environment*, 106(4):428–448.

Wu, J., 1997, "Economic Status in Poyang Lake Region at Tang and Song Dynasty," *Journal of Shanghai Normal University*, 1:43–50 (in Chinese).

Yu, X. and H. Dou, H., 1999, "Impact of Reclamation of Poyang Lake on Flood and Countermeasures," *Environment Protection*, 10:6–7 (in Chinese).